This is an Accepted Manuscript version of the following article, accepted for publication in:

U. Galfarsoro, A. McCloskey, S. Zarate, X. Hernández and G. Almandoz, "Influence of Manufacturing Tolerances and Eccentricities on the Electromotive Force in Permanent Magnet Synchronous Motors," 2022 International Conference on Electrical Machines (ICEM), 2022, pp. 703-709.

DOI: https://doi.org/10.1109/ICEM51905.2022.9910917

Influence of Manufacturing Tolerances and Eccentricities on the Electromotive Force in Permanent Magnet Synchronous Motors

Unai Galfarsoro, Alex McCloskey, Sergio Zarate, Xabier Hernández, Gaizka Almandoz, Member, IEEE

***Abstract* – Eccentricity is a common error in electric motors, so its diagnosis is an important issue. Therefore, the effect of static and dynamic eccentricities on the harmonics of the frequency spectra of the voltage of a phase is studied.**

In this research, dimensional tolerances of the stator and the rotor are also taken into account. The designs of all pieces have dimensional tolerances, hence their real magnitudes change to a degree from the theoretical values after the manufacturing process. As a result of the finite element simulations, validated by experimental results, the conclusion is that the deviations originated by the manufacturing tolerances produce changes in the amplitudes of some harmonics and also additional and characteristic harmonics in the frequency spectra of the phase voltage. These are not negligible and must be taken into account when robust eccentricity detection procedures are defined. Otherwise, harmonics originated by tolerances and by eccentricities can be misidentified.

***Index Terms* -- Fault detection, Fault diagnosis, Voltage measurement, Permanent magnet machines, Tolerance analysis.**

I. INTRODUCTION

The use of electric motors (EMs) is widespread, and is probably going to increase due to the ongoing success of electric vehicles. Yilmaz [1] states that the main kinds of EMs for plug-in hybrid electric vehicles are induction motors (IMs), permanent magnet synchronous motors (PMSMs), DC motors and switched reluctance motors. IMs and PMSMs are winning importance, and PMSMs are leaders in the market. Yilmaz [1] and Riba et al. [2] remark that PMSMs, compared to IMs, are less reliable and technologically mature.

Therefore, since PMSMs are a mass-produced product with a non-negligible danger of failure, it is justified to research the effect of their design on their reliability. According to Hong et al. [3], bearing faults, eccentricities and demagnetization of the permanent magnets (PMs) are the major causes of failures in PMSMs.

This paper analyzes the effect of static eccentricity (SE) and dynamic eccentricity (DE) by experimental measurements and by simulation, including also the ideal case of without eccentricity (WE). Eccentricity is a crucial defect that generates further magnetic and dynamic problems, torque ripple and unbalanced magnetic pull (UMP) [4], triggering additional vibrations and noise [5]. Hong et al. [3], Nandi et al. [6] and Ebrahimi et al. [7] declare that the lowest eccentricity value to take into account is about 5-10% of the air gap. Manufacturing and installation of the EMs create acceptable inherent eccentricity levels below 5-10%.

The experimental work is based on a modified version of the innovative test bench explained by Galfarsoro et al. in [8]. In this test bench SE is generated mounting the stator on a piezoelectric force sensor and supporting the rotor separately, as done by Chen et al. [9], Lee et al. [10] and Dorrell et al. [11]. The generation of SE is possible with this decoupling of the stator and the rotor. A second mechanism is incorporated into the test bench to create DE, by means of a rotor held by a shaft composed of two eccentric pieces that rotate between them [8]. Among other signals, the three electromotive forces (EMF) are determined through the measurement of the three phase voltages.

Regarding simulations, the finite element (FE) method is used to calculate the magnetic flux generated by eccentricities.

Faraday's law of electromagnetic induction states that the EMF is given by the rate of change of the magnetic flux. Therefore, the experimental EMF and the simulated magnetic flux are related and can be compared because they have the same frequency content. The followed methodology is analogue to the one followed by Galfarsoro et al. in [12].

The originality of this study is that dimensional tolerances of the rotor and the stator are considered. All pieces have dimensional tolerances in their designs and their real magnitudes vary to some extend from the theoretical values after the manufacturing process. In the assembly process, in which all pieces of the EM are mounted together, the deviations of dimensions of all pieces are combined giving a final result that is not easy to predict unless a statistical tolerance analysis is carried out. This dimensional irregularities cause changes in the phase voltage of PMSMs, which may not be negligible compared to those that arise due to eccentricities, and thus have to be separated from the fault indicators to detect SE and DE.

Bramerdorfer [13] has carried out tolerance analysis for EM design optimization by statistical calculations, and observed as example the cogging torque and back-EMF sensitivity of an interior PMSM regarding changes in the material characteristics as well as a change in the PMs temperature. The results clearly indicate that the tolerance analysis is essential for the machine design.

Taran et al. [14] have studied three PM EMs with different configurations for dimensional and material

Orona EIC and the Basque Government (MECOVA ZL-2017/00457, MECOVA ZL-2018/00503 and MECOVA ZL-2019/00554) funded this research.

U. Galfarsoro, A. McCloskey, S. Zarate and G. Almandoz are with Mondragon Unibertsitatea, Mondragon, 20500, Spain (e-mail: ugalfarsoro@mondragon.edu, amccloskey@mondragon.edu, szarate@mondragon.edu, galmandoz@mondragon.edu).

X. Hernández is with Orona EIC, Hernani, 20120, Spain (e-mail: xhernandez@orona-group.com).

tolerances, by FE simulation and by experimental measurements. A tolerance of ± 0.1 mm, considered typical for laser cutting prototyping, is considered for eleven geometrical input design variables. Additionally, a ± 5% is considered for the PM remanence in order to account for possible variations both in the material grade and in the external magnetization. The effect of SE on the amplitude of the time signal of the back-EMF and cogging torque of an axial flux PM motor is analyzed. The conclusion is that variations in time signals are too small to have a sensitive enough method, and further studies based on frequency harmonics and side bands are suggested.

According to [14], a systematic study of dimensional and material tolerances is of the utmost importance in the process of designing and manufacturing an EM.

However, no papers that deeply study the influence of eccentricity and manufacturing dimensional tolerances of the rotor and the stator on the phase voltages of PMSMs have been found.

Therefore, the objective of this research is to study experimentally and by simulation the influence of the manufacturing tolerances of the rotor and the stator on the spectra of the phase voltage with SE and DE. To achieve this objective, the real dimensions of the rotor and the stator are measured to assess their values. In addition, several SE and DE values are generated. SE and DE coexist in real EMs, but are studied separately in this paper to simplify the analysis. Comparing experimental and simulation results, the aim is to obtain a good correlation, and as a result evaluate the independent influence of manufacturing tolerances and eccentricities on phase voltages.

II. Analyzed Cases

In experimental measurements the PMSM under study has certain rotor and stator manufacturing dimensions that cannot be changed. Therefore, the study of manufacturing tolerances was carried out with only the initial values, and the changed variables were SE and DE.

In FE simulations the rotor and the stator were first simulated with the theoretical ideal dimensions, varying SE and DE. Then the experimentally measured real dimensions were implemented independently into the rotor, the stator, and both rotor and stator, varying SE and DE in each case.

III. Experimental Measurements of Dimensions

A. Measurement of the remanent magnetic field of magnets

Before mounting the PMs on the rotor, they were magnetized carefully and their magnetization levels were measured using a magnetic characterizer one by one to minimize the effect of their dispersion. The biggest deviation of the magnetization level of one magnet from the mean magnetization level was only 0.26%.

B. Measurement of critical dimensions

The theoretical diameters of the teeth of the stator and the poles of the rotor are known from their drawings (see Table V for the main specifications of the PMSM under test). However, dimensions of parts vary according to manufacturing tolerances. Thus, both diameters were measured on the manufactured PMSM and these real dimensions were used later when the geometry of the FE model was built.

1) Measurement of the Qs = 36 teeth of the stator:

The stator was positioned on the table of a three-dimensional coordinate measuring machine (CMM) and its inner cylindrical bore formed by the teeth was measured (Fig. 1). The diameter of each one of the *Qs* = 36 teeth was measured in 16 points by a contact probe, having a total of 36 x 16 = 576 measured points. Next, the mean of the 16 values was calculated for each tooth and taken as the nominal value of the diameter of the tooth (see these results in Table I). The relative error of Table I was calculated relative to the air gap of 1 mm. Results suggested that deviations of the real diameters of the teeth from the theoretical diameters exceeded values of 5% in most cases and even values of 11% for some teeth. Taking into account that values of eccentricity in the range of 5-10% are considered as residual [3][6][7], the measured values were close or even out of the upper suggested limit.

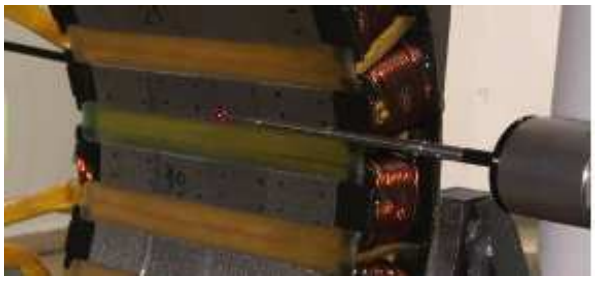

Fig. 1. Measurement of the teeth of the stator in a three-dimensional coordinate measuring machine

TABLE I
TRUE VALUES OF THE DIAMETERS OF THE TEETH OF THE STATOR, MEASURED IN A THREE-DIMENSIONAL COORDINATE MEASURING MACHINE: CALCULATIONS BASED ON MEAN VALUES FOR EACH TOOTH (ONLY VALUES OF 1 OUT OF 3 TEETH ARE SHOWN FOR CONCISENESS)

Tooth number	Mean diameter (mm)	Absolute error (mm)	Relative error (%)	
1	221,956	-0,044	-4,41%	
4	222,053	0,053	5,29%	
7	222,093	0,093	9,25%	
10	221,890	-0,110	-10,99%	Minimum diameter
13	222,063	0,063	6,27%	
16	222,114	0,114	11,45%	Maximum diameter
19	221,917	-0,083	-8,32%	
22	222,080	0,080	8,02%	
25	222,104	0,104	10,42%	
28	221,890	-0,110	-10,98%	
31	222,046	0,046	4,55%	
34	222,104	0,104	10,44%	

Nevertheless, if calculations were based on individual points measured in all teeth, deviations from theoretical diameter values were even bigger, as shown in Table II.

TABLE II
TRUE VALUES OF THE DIAMETERS OF THE TEETH OF THE STATOR, MEASURED IN A THREE-DIMENSIONAL COORDINATE MEASURING MACHINE. CALCULATIONS BASED ON MEAN VALUES FOR EACH TOOTH VS. CALCULATIONS BASED ON INDIVIDUAL POINTS MEASURED IN ALL TEETH

Calculations based on mean values for each tooth		Calculations based on individual points measured in all teeth	
Maximum diameter (mm)	Minimum diameter (mm)	Maximum diameter (mm)	Minimum diameter (mm)
222,114	221,890	222,269	221,819
Absolute error (mm)	Absolute error (mm)	Absolute error (mm)	Absolute error (mm)
0,114	-0,110	0,269	-0,181
Relative error (%)	Relative error (%)	Relative error (%)	Relative error (%)
11,45%	-10,99%	26,92%	-18,09%
Absolute peak-peak error (mm)		Absolute peak-peak error (mm)	
0,224		0,450	
Relative error (%)		Relative error (%)	
22,44%		45,01%	

2) Measurement of the p = 15 pole pairs of the rotor:

The rotor was positioned on its shaft in the PMSM and its outer cylinder was measured using a dial indicator (Fig. 2). Each of the $2p = 30$ poles was measured in 16 points, having a total of 30 x 16 = 480 measured points. Next, the mean of the 16 values was calculated and taken as the nominal deviation of the pole from the theoretical diameter value (see these results in Table III). Results suggest that deviations of the real diameters of the poles from the theoretical diameters were small, much smaller than for the bore of the stator, and inside the range of 5-10% mentioned beforehand as residual for eccentricity [3][6][7]. In spite of their small value, they were taken into account in the FE model.

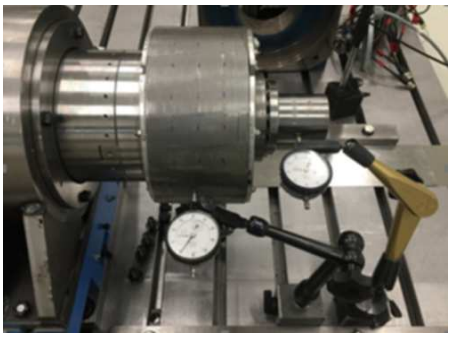

Fig. 2. Measurement of the poles of the rotor by means of dial indicators

TABLE III
TRUE VALUES OF THE DIAMETERS OF THE POLES OF THE ROTOR, MEASURED WITH DIAL INDICATORS: CALCULATIONS BASED ON MEAN VALUES FOR EACH POLE (ONLY VALUES OF 1 OUT OF 3 POLES ARE SHOWN FOR CONCISENESS)

Pole number	Absolute error (mm)	Relative error (%)	
1	0,0087	0,87%	
4	-0,0061	-0,61%	
7	-0,0114	-1,14%	
10	-0,0131	-1,31%	
13	0,0036	0,36%	
16	0,0131	1,31%	
19	-0,0058	-0,58%	
22	-0,0304	-3,04%	Minimum diameter
25	-0,0042	-0,42%	
28	0,0217	2,17%	Maximum diameter

IV. EXPERIMENTAL TEST BENCH

The experimental test bench is based on the concept explained by Galfarsoro et al. [8]. In that study a PMSM with a decoupled rotor and stator was designed and built, enabling the generation of any value of SE and/or DE in a continuous and controlled way. Among other sensors, the test bench was equipped with three Testec 15101 active differential probes to measure the three phase voltages. Results obtained from the measured signals showed that the test bench was suitable to generate SE and/or DE, and to be used to measure different variables to diagnose faults in EMs.

In the present study the abovementioned test bench is connected to a second EM (Fig. 3). The second EM drives the PMSM under test so that it works in open circuit. The objective is to avoid the influence of the control on the PMSM under test, since the control can inject harmonics in the current that are later seen in other measured variables, modifying the effect of the defects (tolerances and eccentricities) analyzed.

Regarding control, the second EM is fed by an inverter, which controls the chosen constant speed. The speed controller is tuned so as to have low speed ripple.

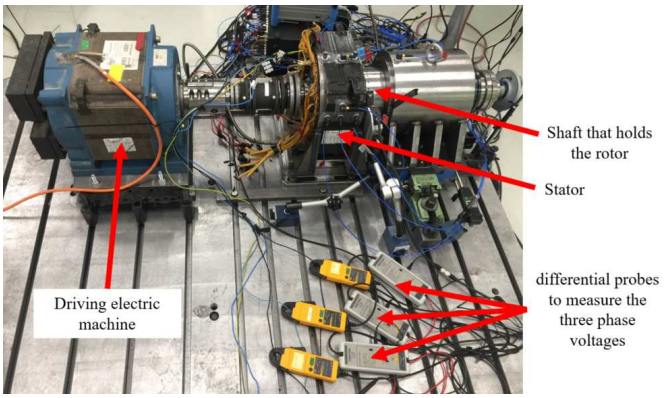

Fig. 3. Experimental test bench for the measurements of the voltages of the three phases

V. ELECTROMAGNETIC FE SIMULATIONS

A. Analyzed cases

Three eccentricity cases were considered in the FE simulations: WE, with SE and with DE. Within each of these three cases, four kinds of tolerances were simulated: 1) Without tolerance (both rotor and stator with the theoretical dimensions, that is, the ideal case); 2) With only rotor tolerances; 3) With only stator tolerances; 4) With both rotor and stator tolerances.

B. Description of the electromagnetic FE simulations

As explained before, the EM has manufacturing tolerances that cannot be disregarded. Referring to the diameters of the poles of the rotor, in order to create the geometry easier, all the poles had the same diameter and the magnet associated to each pole had a correction factor to take into account the different air gap of each pole. Therefore, each magnet had its particular remanence according to the diameter of its pole. The stator teeth had the experimentally measured real dimensions, hence not all the teeth were equal. The eccentricity grade modeled was 55% of the air gap. For each simulation the magnitude of the flux of phase A was

calculated.

VI. RESULTS FOR STATIC ECCENTRICITY

A. *Results of the electromagnetic FE simulations*

Fig. 4 shows the simulated spectra of the magnetic flux of phase A, with both rotor and stator real dimensions. All the spectra in this paper are given in harmonics of the electric frequency. Blue peaks of electric orders correspond to the spectrum WE, and red peaks of electric orders to the spectrum with 55% SE. The conclusion is that electric orders 3, 5, 7, etc. (odd electric orders) change, but those changes do not show a clear trend. Additional harmonics as 0.6 and 1.4 show negligible changes. Amplitudes of odd electric orders are significantly higher so that the changes in the additional harmonics are not noticeable. In addition, new sideband harmonics arise with SE. Fig. 5 displays zoomed two of these frequency components to show that those sidebands $\pm 1/p$ appear around harmonics such as 0.6, which corresponds to the electric order $(p - 2t_p)/p$, p being the number of pole pairs and t_p the machine periodicity. Otherwise, no sidebands arise around electric order 1.

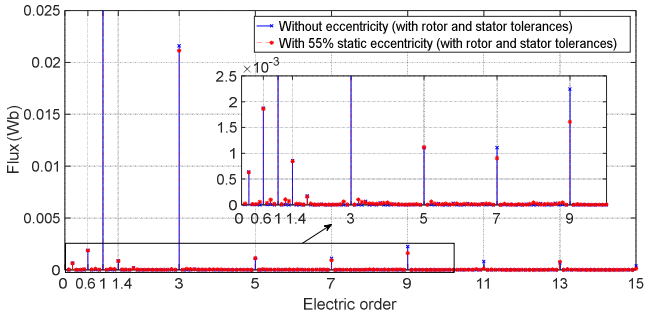

Fig. 4. FFT of the simulated flux of phase A for an increasing value of static eccentricity. Rotor and stator with tolerances

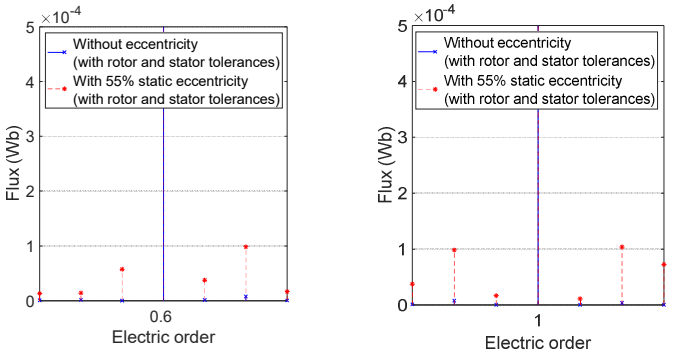

Fig. 5. FFT of the simulated flux of phase A for an increasing value of static eccentricity. Rotor and stator with tolerances. Zoom of electric orders 0.6 (left) and 1 (right)

Fig. 4 shows the influence of SE in the magnetic flux of phase A with rotor and stator tolerances. In Fig. 6 the comparison of WE and with SE cases is presented without rotor and stator tolerances. In both cases the same odd electric harmonics appear, but the amplitudes of those harmonics change with eccentricity. The shape of the wave changes increasing some harmonics and decreasing others, so no pattern can be stablished.

In Fig. 7 the effect of each of the tolerances on SE is separately plotted. The yellow curve, which corresponds to the case with stator tolerances, shows the same harmonics as for the cases without tolerances (Fig. 6). Amplitudes may change, but no new harmonic arises. In contrast, rotor tolerances (green curve) induce new harmonics. Those new harmonics are multiples of twice t_p divided p and their sidebands $1/p$.

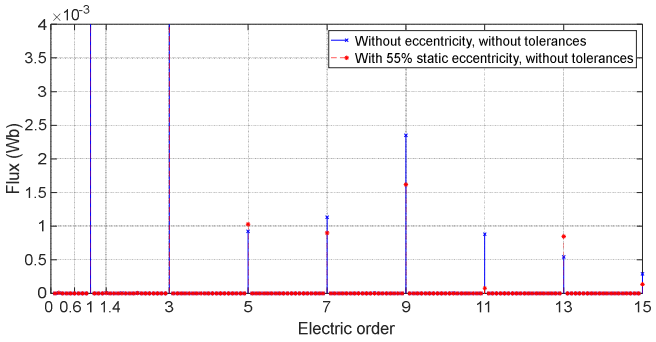

Fig. 6. Effect of static eccentricity on the FFT of the simulated flux of phase A, without tolerances

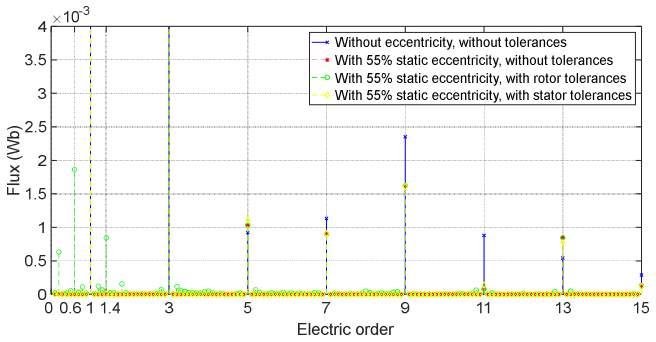

Fig. 7. Effect of tolerances on the FFT of the simulated flux of phase A, with static eccentricity

B. *Results of the experimental measurements*

The Fast Fourier Transforms (FFTs) of the measured voltages of phase A for increasing values of SE are shown in Fig. 8. The results confirm that SE changes the frequency content of the voltages of phase A, increasing some characteristic orders and decreasing others. The experimental measurements were carried out in a machine with rotor and stator tolerances. Therefore, comparison in Fig. 8 corresponds to the comparison of simulations in Fig. 4. In both cases, the odd electric harmonics and their sidebands of $2t_p/p$ are significant. In addition, all those harmonics show $1/p$ sidebands. All these were observed at the FE results.

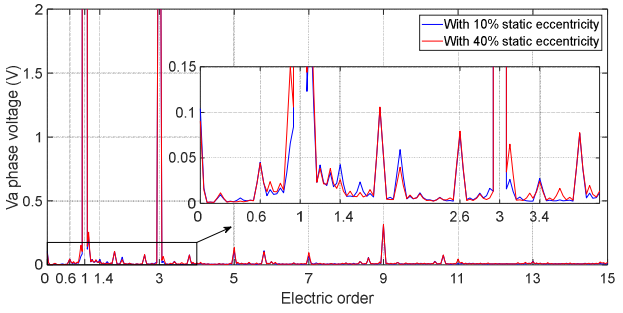

Fig. 8. FFT of the experimental voltage of phase A for an increasing value of static eccentricity

VII. RESULTS FOR DYNAMIC ECCENTRICITY

A. *Results of the electromagnetic FE simulations*

Fig. 9 shows the simulated spectra of the magnetic flux of phase A with both rotor and stator real dimensions. Blue peaks of electric orders correspond to the spectrum WE, and red peaks of electric orders to the spectrum with 55% SE. The conclusion is that electric orders 3, 5, 7, etc. (odd electric orders) change, but those change as for the SE, but do not show a clear trend. Additional harmonics as 0.6 and 1.4 show significant changes, more noticeable than for SE. In addition, new sideband harmonics arise with DE.

Fig. 10 displays zoomed two of these frequency components to show that those sidebands $\pm 1/p$ appear around harmonic 1. Otherwise, no sidebands arise around electric order 0.6. These results show the opposite of that observed for the SE. Thus, those sidebands allow to distinguish between SE and DE.

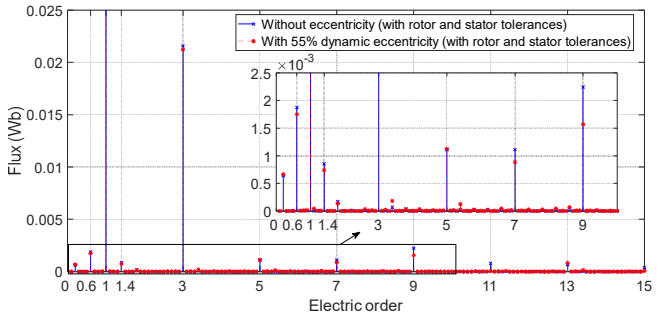

Fig. 9. FFT of the simulated flux of phase A for an increasing value of dynamic eccentricity. Rotor and stator with tolerances

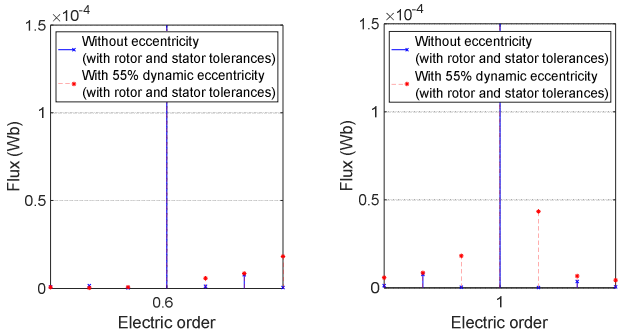

Fig. 10. FFT of the simulated flux of phase A for an increasing value of dynamic eccentricity. Rotor and stator with tolerances. Zoom of electric orders 0.6 (left) and 1 (right)

Fig. 9 takes into account the simultaneous effect of rotor and stator tolerances in the flux of phase A with DE. In Fig. 11 the results without tolerances are presented. The odd electric orders appear with and without DE, but their amplitudes change. In addition, side bands of multiples of twice t_p appear with DE.

In Fig. 12 the effect of each of the tolerances on DE is plotted. The red and green curves, which correspond to DE without tolerances and DE with rotor tolerances, show the same harmonics with changes in their amplitudes. Rotor tolerances have the effect of an increased DE. In fact, it is observed that the influence in the amplitude of those harmonics is significantly bigger for rotor tolerances than for the dynamic eccentricity. When stator tolerances are added (yellow curve) new harmonics arise as sidebands ($\pm 1/p$) around the odd electric harmonics.

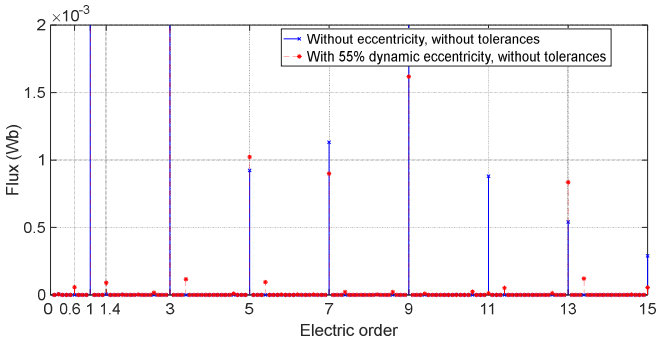

Fig. 11. Effect of dynamic eccentricity on the FFT of the simulated flux of phase A, without tolerances

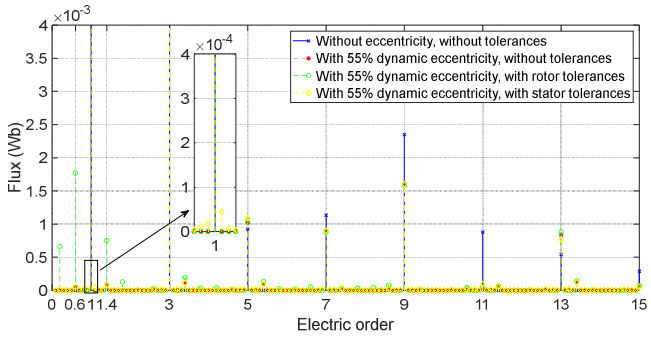

Fig. 12. Effect of tolerances on the FFT of the simulated flux of phase A, with dynamic eccentricity

B. *Results of the experimental measurements*

The FFTs of the measured voltages of phase A for increasing values of DE are shown in Fig. 13. These results confirm that DE also changes the frequency content of the voltages of phase A, increasing some characteristic orders and decreasing others. The experimental measurements were carried out in a machine with rotor and stator tolerances. Therefore, comparison in Fig. 13 corresponds to the comparison of simulations in Fig. 9. In both cases, the odd electric harmonics and their sidebands of $2t_p/p$ are significant. In addition, the odd harmonics show sidebands $1/p$. The simulations showed all these harmonics. It needs to be pointed out that the sidebands $1/p$ of the harmonics $(p \pm 2t_p)/p$ are not observed. This is relevant, since those harmonics are indicators of SE.

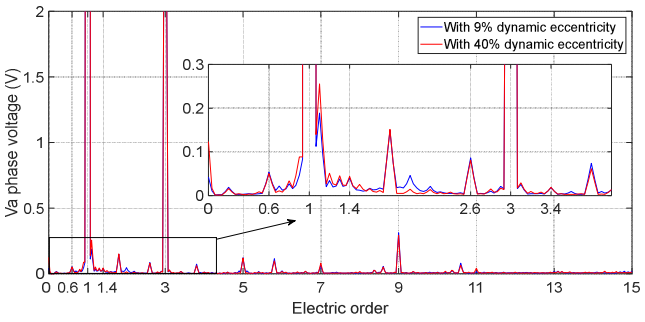

Fig. 13. FFT of the experimental voltage of phase A for an increasing value of dynamic eccentricity

VIII. Summary of FE simulation results

The main orders in the spectra of the results of the simulations are summarized in Table IV for the PMSM WE, with SE and with DE. These orders are shown as mechanical orders for simplicity (divide all values by p to obtain electric orders). The conclusion from these FE simulations is that SE and DE generate new peaks in the spectra of magnetic flux of a phase, and therefore in the electromotive force induced per phase. Those peaks depend on the dimensional tolerances of the rotor and the stator.

TABLE IV
MAIN MECHANICAL ORDERS IN THE FLUX OF A PHASE WITHOUT ECCENTRICITY, WITH STATIC ECCENTRICITY AND WITH DYNAMIC ECCENTRICITY, DEPENDING ON TOLERANCE TYPE

Without eccentricity			
Ideal	Rotor tolerance	Stator tolerance	Rotor + Stator tolerance
$p\cdot(2u-1)$	$p\cdot(2u-1)$ $p\cdot(2u-1)\pm 2t_p\cdot v$	$p\cdot(2u-1)$	$p\cdot(2u-1)$ $p\cdot(2u-1)\pm 2t_p\cdot v$
Static eccentricity			
Ideal	Rotor tolerance	Stator tolerance	Rotor + Stator tolerance
$p\cdot(2u-1)$	$p\cdot(2u-1)$ $p\cdot(2u-1)\pm 2t_p\cdot v$ $p\cdot(2u-1)\pm 2t_p\cdot v\pm 1\cdot w$ $p\cdot(2u-1)\pm 1\cdot w$	$p\cdot(2u-1)$	$p\cdot(2u-1)$ $p\cdot(2u-1)\pm 2t_p\cdot v$ $p\cdot(2u-1)\pm 2t_p\cdot v\pm 1\cdot w$ $p\cdot(2u-1)\pm 1\cdot w$
Dynamic eccentricity			
Ideal	Rotor tolerance	Stator tolerance	Rotor + Stator tolerance
$p\cdot(2u-1)$	$p\cdot(2u-1)$ $p\cdot(2u-1)\pm 2t_p\cdot v$	$p\cdot(2u-1)$ $p\cdot(2u-1)\ \pm 1\cdot w$	$p\cdot(2u-1)$ $p\cdot(2u-1)\pm 2t_p\cdot v$ $p\cdot(2u-1)\pm 1\cdot w$

$t_p = \mathrm{GCD}(Qs, p)$ is the periodicity of the winding pattern (that is, the number of its symmetries)

$u = 0,1,2,3\ldots$, $v = 0,1,2,3\ldots$ and $w = 0,1,2,3\ldots$ are integer numbers

IX. Conclusions

The phase voltage of a PMSM was measured experimentally and the flux of a phase was calculated by FE simulation with similar trends in results. The main conclusion is that the frequency components of the phase voltage with eccentricity depend not only on the type and level of eccentricity, but also on the tolerances of the dimensions of the rotor and the stator and on the tolerances of the magnetization levels of the magnets. An ideal machine would only show odd electric harmonics, but tolerances induce many other frequency components. Some of the biggest peaks are due to rotor tolerances $(p\pm 2t_p)/p$ and stator tolerances combined with dynamic eccentricity generate additional sidebands. Therefore, a robust eccentricity detection procedure must consider the manufacturing tolerances, as the amplitudes of the harmonics of the phase voltage change with them. However, the combination of tolerances and eccentricities allows discerning between static and dynamic eccentricity, because they cause different frequency components. The main difference are the sidebands of the harmonics $(p\pm 2t_p)/p$, which only were observed with static eccentricities. The drawback is that the amplitudes of these harmonics are low and background noise may make it difficult to identify them. Otherwise, the biggest frequency components change with tolerances and eccentricities, but no clear trends were observed. It is expected that those harmonics may increase or decrease depending on the design of the machine.

X. Appendix

TABLE V
PMSM UNDER TEST MAIN SPECIFICATIONS

Pole pairs (p)	15
Number of slots of the stator (Qs)	36
Rotor outer diameter / length	220 mm / 100 mm
Stator inner diameter / length	222 mm / 100 mm
Air gap	1 mm
Rated speed	96 rpm

XI. Acknowledgment

The authors gratefully acknowledge the contributions of B. Arregi, P. Iruretagoiena, E. Lizarazu, I. Badias, J.M. Iriondo, A. Villar, J. Maskariano, L. Azpitarte, A. Garate, G. Aretxaga, J. Larrañaga, I. Ezpeleta, A. Arana, I. Eraña, and others, for their work on the design, manufacturing, assembly and final tuning of the test bench.

Thanks also to Brüel & Kjær for their support with the multi-channel data acquisition and analysis system made up of LAN-XI front-ends and BK Connect software.

XII. References

[1] M. Yilmaz, "Limitations/capabilities of electric machine technologies and modeling approaches for electric motor design and analysis in plug-in electric vehicle applications," *Renewable and Sustainable Energy Reviews*, vol. 52, pp. 80–99, 2015.

[2] J. R. Riba, C. López-Torres, L. Romeral, and A. Garcia, "Rare-earth-free propulsion motors for electric vehicles: A technology review," *Renewable and Sustainable Energy Reviews*, vol. 57, pp. 367–379, May 2016.

[3] J. Hong, S. Park, D. Hyun, T. Kang, S. B. Lee, C. Kral, and A. Haumer, "Detection and classification of rotor demagnetization and eccentricity faults for PM synchronous motors," *IEEE Transactions on Industry Applications*, vol. 48, no. 3, pp. 923–932, May 2012.

[4] *VDI 3839-5:2001. Instructions on measuring and interpreting the vibration of machines - Typical vibration patterns with electrical machines*. VDI (The Association of German Engineers), 2001.

[5] W. le Roux, R. G. Harley, and T. G. Habetler, "Detecting Rotor Faults in Low Power Permanent Magnet Synchronous Machines," *IEEE Transactions on Power Electronics*, vol. 22, pp. 322–328, Jan. 2007.

[6] S. Nandi, H. A. Toliyat, and X. Li, "Condition Monitoring and Fault Diagnosis of Electrical Motors - A Review," *IEEE Transactions on Energy Conversion*, vol. 20, pp. 719–729, Dec. 2005.

[7] B. M. Ebrahimi, M. J. Roshtkhari, J. Faiz, and S. V. Khatami, "Advanced eccentricity fault recognition in permanent magnet synchronous motors using stator current signature analysis," *IEEE Transactions on Industrial Electronics*, vol. 61, no. 4, pp. 2041–2052, Apr. 2014.

[8] U. Galfarsoro, A. McCloskey, X. Hernandez, G. Almandoz, S. Zarate, and X. Arrasate, "Eccentricity detection procedure in electric motors by force transducer and search coils in a novel experimental test bench," in *12th IEEE International Symposium on Diagnostics for Electrical Machines, Power Electronics and Drives (SDEMPED 2019)*, 2019, pp. 220–226.

[9] X. Chen, Z. Deng, J. Hu, and T. Deng, "An analytical model of unbalanced magnetic pull for PMSM used in electric vehicle: Numerical and experimental validation," *International Journal of*

Applied Electromagnetics and Mechanics, vol. 54, no. 4, pp. 583–596, 2017.

[10] C.I. Lee and G. H. Jang, "Experimental measurement and simulated verification of the unbalanced magnetic force in brushless DC motors," *IEEE Transactions on Magnetics*, vol. 44, no. 11, pp. 4377–4380, 2008.

[11] D. Dorrell and A. Smith, "Calculation and measurement of unbalanced magnetic pull in cage induction motors with eccentric rotors. II. Experimental investigation," *IEE Proceedings-Electric Power Applications*, vol. 143, no. 3, pp. 202–210, 1996.

[12] U. Galfarsoro, A. Mccloskey, S. Zarate, X. Hernandez, and G. Almandoz, "Influence of manufacturing tolerances and eccentricities on the unbalanced magnetic pull in permanent magnet synchronous motors," *IEEE Transactions on Industry Applications*, 2022.

[13] G. Bramerdorfer, "Tolerance Analysis for Electric Machine Design Optimization: Classification, Modeling and Evaluation, and Example," *IEEE Transactions on Magnetics*, vol. 55, no. 8, pp. 1–9, 2019.

[14] N. Taran, V. Rallabandi, D. M. Ionel, P. Zhou, M. Thiele, and G. Heins, "A systematic study on the effects of dimensional and materials tolerances on permanent magnet synchronous machines based on the IEEE Std 1812," *IEEE Transactions on Industry Applications*, vol. 55, no. 2, pp. 1360–1371, 2018.

XIII. BIOGRAPHIES

Unai Galfarsoro was born in Saint-Jean-de-Luz, France. He received the B.Sc. and M.Sc. degrees in Mechanical Engineering and Industrial Engineering from Mondragon Unibertsitatea in 1991 and 2004 respectively. He developed his Ph.D. thesis about fault diagnosis of electrical machines in Mondragon Unibertsitatea.

Since 1993, he has been with the Acoustics and Vibrations Group of the Mechanics and Manufacturing department of the Faculty of Engineering of Mondragon Unibertsitatea, where he is currently a Lecturer and Researcher. His current research interests include noise source identification, and electrical machines diagnosis. He has participated in a number of research projects in the fields of elevator drives, household appliances, machine tools, etc.

Alex McCloskey was born in Dublin, Ireland. He received the B.Sc. and M.Sc. degrees in Mechanical Engineering and Industrial Engineering from Mondragon Unibertsitatea in 2009 and 2012 respectively. He developed his Ph.D. thesis about vibrations of electrical machines in Mondragon Unibertsitatea.

Since 2016, he has been with the Acoustics and Vibrations Group of the Mechanics and Manufacturing department of the Faculty of Engineering of Mondragon Unibertsitatea, where he is currently a Lecturer and Researcher. His current research interests include electrical machines design and diagnosis. He has participated in a number of research projects in the fields of elevator drives and railway traction.

Sergio Zarate was born in Vitoria-Gasteiz, Spain. He received the B.Sc., M.Sc. and Ph.D. degrees in electrical engineering at Mondragon Unibertsitatea, Mondragon, Spain, in 2012, 2014 and 2018, respectively.
Since 2018, he has been with the Electronics department of the Faculty of Engineering of Mondragon Unibertsitatea, where he is currently a Lecturer and Researcher. His current research interests include drives, electrical machines vibration and permanent magnet machine design and optimization.

Xabier Hernández was born in Pasaia, Spain. He received the B.Sc. and M.Sc. degrees in Mechanical Engineering and Industrial Engineering from Mondragon Unibertsitatea in 2008 and 2011 respectively.

Since 2011, he works in Orona S. Coop. where he currently is in charge of the Vibroacoustics research team. During this period, he has participated in several industrial research projects. His current research interests include electrical machines design, vibroacoustic design and diagnosis.

Gaizka Almandoz was born in Arantza, Spain. He received the B.Sc. and Ph.D. degrees in electrical engineering at Mondragon Unibertsitatea, Mondragon, Spain, in 2003 and 2008, respectively.

Since 2003, he has been with the Electronics, Faculty of Engineering, Mondragon Unibertsitatea, where he is currently an Associate Professor. His current research interests include electrical machine design, modelling and control. He has participated in various research projects in the fields of wind energy systems, elevator drive and railway traction.